J|A|C|S
ARTICLES
Published on Web 05/18/2006

Conformationally Gated Photoinduced Processes within Photosensitizer−Acceptor Dyads Based on Osmium(II) Complexes with Triarylpyridinio-Functionalized Terpyridyl Ligands: Insights from Experimental Study

Philippe P. Lainé,*[,†] Fethi Bedioui,[‡] Frédérique Loiseau,[§] Claudio Chiorboli,[||] and Sebastiano Campagna*[,§]

Contribution from the Laboratoire de Chimie et Biochimie Pharmacologiques et Toxicologiques, CNRS UMR-8601, Université René Descartes, 45 rue des Saints Pères, F-75270, Paris Cedex 06, France; Laboratoire de Pharmacologie Chimique et Génétique, CNRS UMR-8151 + INSERM U-640, École Nationale Supérieure de Chimie de Paris, 11 rue P. et M. Curie, F-75231 Paris Cedex 05, France; Università di Messina, Dipartimento di Chimica Inorganica, Chimica Analitica e Chimica Fisica, Via Sperone 31, I-98166 Messina, Italy, and ISOF-CNR, Sezione di Ferrara, 44100 Ferrara, Italy

Received December 9, 2005; Revised Manuscript Received March 28, 2006; E-mail: philippe.laine@univ-paris5.fr; campagna@unime.it

Abstract: [(ttpy)Os(tpy-ph-TPH_3^+)]$^{3+}$ (**2**), [(ttpy)Os(tpy-xy-TPH_3^+)]$^{3+}$ (**3**), [(ttpy)Os(tpy-ph-$TPH_2(NO_2)^+$)]$^{3+}$ (**4**), and [(ttpy)Os(tpy-xy-$TPH_2(NO_2)^+$)]$^{3+}$ (**5**) are a series of dyads made of an Os(II) bis-tpy complex (tpy = 2,2′:6′,2″-terpyridine) as the photosensitizer (P) and 2,4,6-triarylpyridinium group (TP^+) as the electron acceptor (A). These dyads were designed to form charge-separated states (CSS) upon light excitation. Together with analogous Ru(II) complexes (**7**−**10**), they have been synthesized and fully characterized. We describe herein how intramolecular photoinduced processes are affected when the electron-accepting strength of A (by nitro-derivatization of TP^+) and/or the steric hindrance about intercomponent linkage (by replacing a phenyl spacer by a xylyl one) are changed. Electronic absorption and electrochemical behavior revealed that (i) chemical substitution of TP^+ (i.e., TP^+-NO_2) has no sizable influence on P-centered electronic features, (ii) reduction processes located on TP^+ depend on the intercomponent tilt angle. Concerning excited-state properties, photophysical investigation evidenced that phosphorescence of P is actually quenched in dyads **4** and **5** only. Ultrafast transient absorption (TA) experiments allowed attributing the quenching in *conformationally locked* dyad **5** to oxidative electron transfer (ET) from the ^{3}MLCT level to the TP^+-NO_2 acceptor ($k_{el} = 1.1 \times 10^9$ s^{-1}). For **4**, *geometrically unlocked*, the ^{3}MLCT state was shown to first rapidly equilibrate (reversible energy transfer; $k_{eq} \approx 2 \times 10^9$ s^{-1}) with a ligand centered triplet state before undergoing CSS formation. Thus, the pivotal role of conformation in driving excited-state decay pathways is demonstrated. Also, inner P structural *planarization* as a relaxation mode of the ^{3}MLCT states has been inferred from TA experiments.

1. Introduction

High level of organization is counted among basic features of natural functional assemblies. This finding has contributed to lead to the foundation of the conceptual corpus of supramolecular chemistry,[1a] with the goal to create molecule(s)-based artificial systems functioning as devices.[1b] When such well-defined supermolecules are getting to interact with light in a specific manner to become photochemical molecular devices (PMDs), we are entering the domain of supramolecular photochemistry.[2] Deriving[3] from "classical" inorganic photochemistry,[4,5] supramolecular photochemistry has a share in the advancement of research fields like nanosciences[6,7] (including molecular electronics[8] and photonic[9]) and bioinorganic photochemistry,[10] which are both relevant frameworks for the present work devoted to the design of PMDs capable of handling intramolecular directional photoinduced electron transfer (PET).[11]

† Université René Descartes.
‡ ENSCP.
§ Università di Messina.
|| ISOF−CNR.

(1) (a) Lehn, J.-M. *Angew. Chem., Int. Ed. Engl.* **1988**, *27*, 89−112. (b) Lehn, J.-M. *Angew. Chem., Int. Ed. Engl.* **1990**, *29*, 1304−1319.
(2) (a) Balzani, V. *Tetrahedron* **1992**, *48*, 10443−10514. (b) Balzani, V.; Scandola, F. *Supramolecular Photochemistry*; Ellis Horwood: Chichester, U.K. 1991; Chapter 12. (c) Balzani, V.; Moggi, L.; Scandola, F. in *Supramolecular Photochemistry*; Balzani, V., Ed; D. Reidel Publishing Co.: Dordrecht, The Netherlands, 1987; pp 1−28.
(3) Balzani, V.; Juris, A. *Coord. Chem. Rev.* **2001**, *211*, 97−115.
(4) State-of-the-Art Symposium: Inorganic Photochemistry. Hoffman, M. Z., Ed; *J. Chem. Educ.* **1983**, *60* (special issue).
(5) Meyer, T. J. *Pure Appl. Chem.* **1990**, *62*, 1003−1009.
(6) Balzani, V. *Small* **2005**, *1*, 278−283.
(7) Ballardini, R.; Balzani, V.; Clemente-León, M.; Credi, A.; Gandolfi, M. T.; Ishow, E.; Perkins, J.; Stoddart, J. F.; Tseng, H.-R.; Wenger, S. *J. Am. Chem. Soc.* **2002**, *124*, 12786−12795, and references therein.
(8) Ward, M. D. *J. Chem. Educ.* **2001**, *78*, 321−328.
(9) Coe, B. J.; Curati, N. R. M. *Comments Inorg. Chem.* **2004**, *25*, 147−184.
(10) Szacilowski, K.; Macyk, W.; Drzewiecka-Matuszek, A.; Brindell, M.; Stochel, G. *Chem. Rev.* **2005**, *105*, 2647−2694, and references therein.
(11) Gust, D.; Moore, T. A.; Moore, A. L. *Acc. Chem. Res.* **2001**, *34*, 40−48.

 10.1021/ja058357w CCC: $33.50

Depending on whether light input is viewed as a trigger signal (quantum of information) or as an energy source (to be conveyed or converted), targeted applications are rather directed toward information processing or artificial photosynthesis purposes, respectively.[12]

When dealing with photoinduced processes, "reaction centers" of natural photosynthetic organisms, that perform conversion of solar energy into chemical fuels for their cellular machinery, are benchmark functional assemblies.[11,13−15] Beyond its complexity, order within photosynthetic apparatus has been clearly highlighted thanks to X-ray diffraction which has proved to be a pertinent analytical method to investigate this type of supramolecular assemblies of biological origin.[16] The photosynthetic organization, in which involved photo- and/or redox-active elements were found to be harmoniously set out with utmost precision,[17] presents a hierarchical association between two functions.[18] The first one is specialized in the collection of photons and the funneling of light energy (antenna) while the second one is in charge of the transduction of previously conveyed excitation energy into usable electrochemical potential ("redox energy") by carrying out so-called charge separation (CS). Brought together, structural issues and insights gained from time-resolved spectroscopic experiments have allowed to evidence another analytical grid of photosynthetic organizations, which lies at the energetic level. Indeed, an arrangement of active components according to energy gradients was revealed, that could be superposed on overall spatial orderliness.[19−21] Therefore, key-organization of operative functional assemblies—at least when photoinduced processes are concerned—is actually *dual*, being attached to both spatial and energy layouts.

Design of artificial photochemical charge separation devices, that is, functional models for directional ET more specifically conceived to form charge separated states (CSS) upon light excitation, goes through consideration of the above-identified features.[22−24] So far, two main strategies have been proposed to obtain such hierarchical molecular assemblies integrating the two functions of *antenna* and *CS*. One approach is relying on the use of supports[25] and matrices as rigid host (organizing medium) to fix active components in a predetermined manner. The matrices can either be proteins (using natural apo-proteins according to semi-synthetic strategy[26] or using synthetic tailor-made computationally designed proteins[27]), liposome bilayers,[28] thin films and lamellar solids[29] or purely mineral materials, for example zeolites.[30] For an alternative approach relying on genuine PMDs, components are held together by covalent links,[12−15,31,32] weak supramolecular-interactions[7,33] or even mechanical contacts.[34] The counterpart at the molecular level of dual organization of reference natural functional systems lies in *combined rigidity and chemical variability*.[12−15] *Rigidity* results in structurally well-defined architectures[35,36] while *chemical variability* allows both tuning of electronic properties of subunits and spatial expansion of the supermolecule so as to generate energy gradients (e.g., "redox cascade" for CS). In addition, functional integration is achieved by using a strongly absorbing photosensitizer (P) which also behaves as a primary intramolecular electron donor when photoexcited.

Chart 1. Salient Features of TP^+-derivatized Tpy Ligands

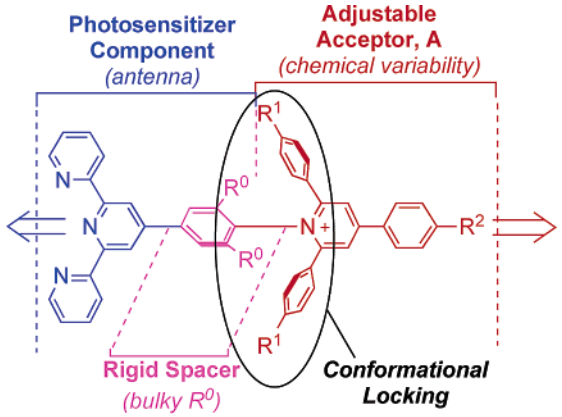

In an effort to exert more accurate control over both structural and electronic features of supermolecules intended to perform photoinduced CS, we have recently proposed to rely on oligopyridyl ligands functionalized with the 2,4,6-triarylpyridinium (TP^+) electron-acceptor group, A (Chart 1).[37] The overall architecture of complexes with 4′-[*p*-(TP^+-derivatized)-phenyl]-2,2′:6′,2″-terpyridine native ligands (tpy-ph-TP^+) is rigid despite possible conformational fluctuations along main single-axis symmetry that gives the rodlike shape to derived supermolecules. Chemical variability results from the possible substitution on

(12) Sauvage, J.-P.; Collin, J.-P.; Chambron, J.-C.; Guillerez, S.; Coudret, C.; Balzani, V.; Barigelleti, F.; De Cola, L.; Flamigni, L. *Chem. Rev.* **1994**, *94*, 993−1019.
(13) Baranoff, E.; Collin, J.-P.; Flamigni, L.; Sauvage, J.-P. *Chem. Soc. Rev.* **2004**, *33*, 147−155.
(14) Kurreck, H.; Huber, M. *Angew. Chem., Int. Ed. Engl.* **1995**, *34*, 849−866.
(15) Wasielewski, M. R. *Chem. Rev.* **1992**, *92*, 435−461.
(16) Deisenhofer, J.; Epp, O.; Miki, K.; Huber, R.; Michel, H. *Nature (London)* **1985**, *318*, 618−624.
(17) Zouni, A.; Witt, H.-T.; Kern, J.; Fromme, P.; Krauss, N.; Saenger, W.; Orth, P. *Nature (London)* **2001**, *409*, 739−743.
(18) Roszak, A. W.; Howard, T. D.; Southall, J.; Gardiner, A. T.; Law, C. J.; Isaacs, N. W.; Cogdell, R. J. *Science* **2003**, *302*, 1969−1972.
(19) Lubitz, W.; Lendzian, F.; Bittl, R. *Acc. Chem. Res.* **2002**, *35*, 313−320.
(20) Hu, X.; Damjanovic, A.; Ritz, T.; Schulten, K. *Proc. Natl. Acad. Sci. U.S.A.* **1998**, *95*, 5935−5941.
(21) Hoff, A. J.; Deisenhofer, J. *Phys. Rep.* **1997**, *287*, 1−247.
(22) Browne, W. R.; O'Boyle, N. M.; McGarvey, J. J.; Vos, J. G. *Chem. Soc. Rev.* **2005**, *34*, 641−663.
(23) Alstrum-Acevedo, J. H.; Brennaman, M. K.; Meyer, T. J. *Inorg. Chem.* **2005**, *44*, 6802−6827.
(24) Chakraborty, S.; Wadas, T. J.; Hester, H.; Schmehl, R.; Eisenberg, R. *Inorg. Chem.* **2005**, *44*, 6865−6878.
(25) Sykora, M.; Maxwell, K. A.; DeSimone, J. M.; Meyer, T. J. *Proc. Natl. Acad. Sci. U.S.A.* **2000**, *97*, 7687−7691.
(26) Hu, Y.-Z.; Takashima, H.; Tsukiji, S.; Shinkai, S.; Nagamune, T.; Oishi, S.; Hamachi, I. *Chem. Eur. J.* **2000**, *6*, 1907−1916.
(27) Cristian, L.; Piotrowiak, P.; Farid, R. S. *J. Am. Chem. Soc.* **2003**, *125*, 11814−11815.
(28) Steinberg-Yfrach, G.; Liddell, P. A.; Hung, S.-C.; Moore, A. L.; Gust, D.; Moore, T. A. *Nature (London)* **1997**, *385*, 239−241.
(29) Hoertz, P. G.; Mallouk, T. E. *Inorg. Chem.* **2005**, *44*, 6828−6840.
(30) Kim, Y.; Lee, H.; Dutta, P. K. *Inorg. Chem.* **2003**, *42*, 4215−4222.
(31) Treadway, J. A.; Chen, P.; Rutherford, T. J.; Keene, F. R.; Meyer, T. J. *J. Phys. Chem. A* **1997**, *101*, 6824−6826.
(32) (a) Klumpp, T.; Linsenmann, M.; Larson, S. L.; Limoges, B. R.; Bürssner, D.; Krissinel, E. B.; Elliott, C. M.; Steiner, U. E. *J. Am. Chem. Soc.* **1999**, *121*, 1076−1087. (b) Ryu, C. K.; Wang, R.; Schmehl, R. H.; Ferrere, S.; Ludwikow, M.; Merkert, J. W.; Headford, C. E. L.; Elliott, C. M. *J. Am. Chem. Soc.* **1992**, *114*, 430−438.
(33) (a) Haider, J. M.; Pikramenou, Z. *Chem. Soc. Rev.* **2005**, *34*, 120−132. (b) Myles, A. J.; Branda, N. R. *J. Am. Chem. Soc.* **2001**, *123*, 177−178. (c) Ward, M. D.; White, C. M.; Barigelletti, F.; Armaroli, N.; Calogero, G.; Flamigni, L. *Coord. Chem. Rev.* **1998**, *171*, 481−488.
(34) Dürr, H.; Bossmann, S. *Acc. Chem. Res.* **2001**, *34*, 905−917.
(35) It's worth noting that by limiting ill-defined intramolecular changes, such rigid architectures also facilitate theoretical modeling and understanding of photophysical behavior.
(36) Vögtle, F.; Frank, M.; Nieger, M.; Belser, P.; Von Zelewsky, A.; Balzani, V.; Barigelletti, F.; De Cola, L.; Flamigni, L. *Angew. Chem., Int. Ed. Engl.* **1993**, *32*, 1643−1646.
(37) (a) Lainé, P.; Bedioui, F.; Amouyal, E.; Albin, V.; Berruyer-Penaud, F. *Chem. Eur. J.* **2002**, *8*, 3162−3176. (b) Lainé, P.; Bedioui, F.; Ochsenbein, P.; Marvaud, V.; Bonin, M.; Amouyal, E. *J. Am. Chem. Soc.* **2002**, *124*, 1364−1377. (c) Lainé, P.; Amouyal, E. *Chem. Commun.* **1999**, 935−936.

Chart 2. Label of the Molecules Studied. Counteranions Are BF_4^- for Organic Models and PF_6^- for Complexes

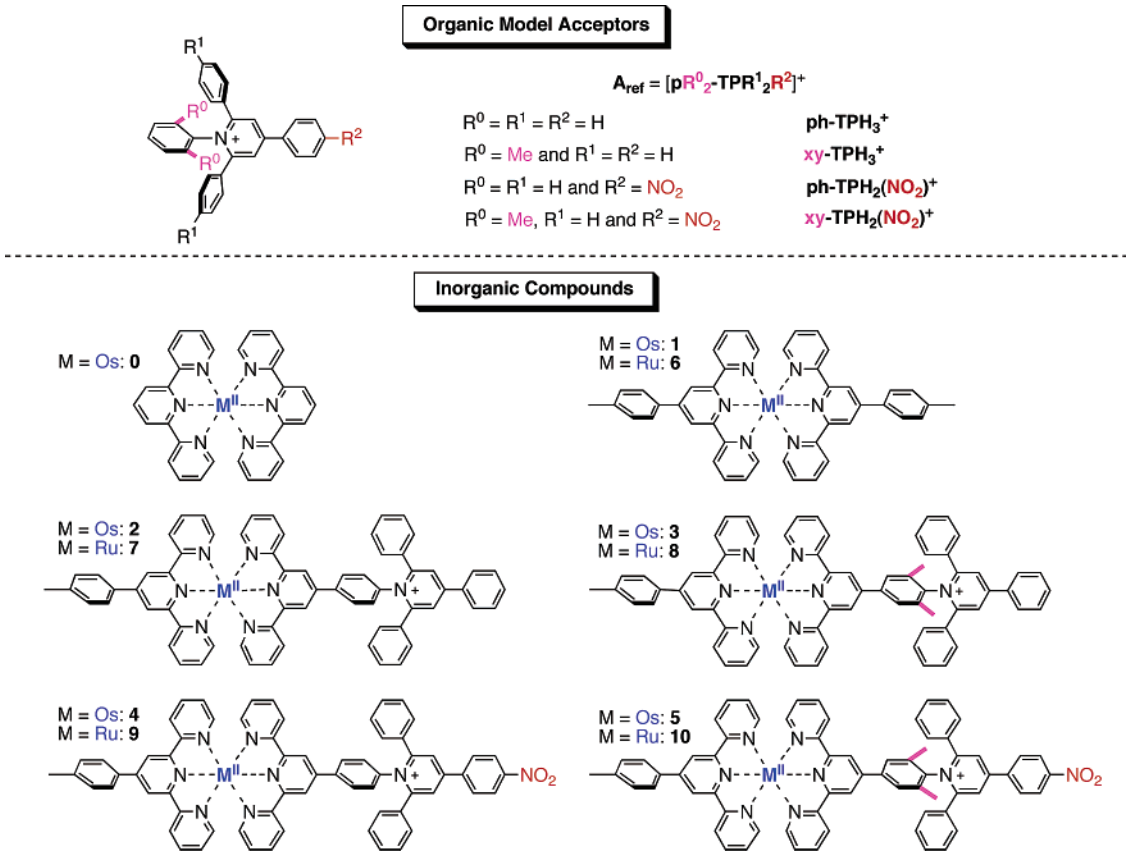

the TP^+ unit (R^1, R^2), choice of d^6 transition metal cation (M) forming the $[M(tpy)_2]$ bis-tpy core of the photosensitizer (P) and the choice of ancillary ligand which can bear an electron-donating group. The structure is potentially extendable (via the R^2 position) to form a so-called "redox cascade" for long-range PET and long-lived CSS. When the chemical variability concerns the bridging element (linker) such as R^0 substituents of the spacer (Chart 1), the level of conformational restriction is first tuned. There exists however a strong correlation between structural and electronic properties as the TP^+-derivatized organic ligand is potentially fully conjugated. This relationship is a supplementary reason for finely controlling the intramolecular geometry. Indeed, when designing PMDs, one has to ensure that electronic identity of various active components is retained[2,12] so as to perform vectorial ET by hopping from one discrete state to another[38,39] according to a predetermined energy gradient referred to as "redox cascade". To do so, we[37] and others[39−46] have relied on a "*geometrical decoupling*" strategy to minimize adverse intercomponent electronic coupling, at least as far as $\pi-\pi$ interactions, which have by far the largest contribution to electronic communication, are concerned. Such a geometrical decoupling consists in forcing connected subunits to adopt a perpendicular conformation by increasing steric hindrance about the intercomponent linkage. Here, the structural effect is mainly originating from the bulky phenyl substituents ortho to the $N_{pyridinio}$ atom of TP^+ (Chart 1) and has been shown to be effective in the ground state.[37,39]

A recent theoretical analysis[47] of the electronic behavior of the reference photosensitizer complex $[Os(ttpy)_2]^{2+}$ (**1**; ttpy is the 4′-tolyl-tpy, also used as ancillary ligand in dyads; Chart 2) and nonoptimized native dyad $[(ttpy)Os(tpy\text{-}ph\text{-}TPH_3^+)]^{3+}$ (**2**) represented in Chart 2, has shown that a structural reorganization is very likely to occur in the excited-state despite molecular rigidity, as a consequence of (photoinduced) charge redistribution. Such geometrical changes have already been observed[48−53]

(38) Berlin, Y. A.; Hutchinson, G. R.; Rempala, P.; Ratner, M. A.; Michl, J. *J. Phys. Chem. A.* **2003**, *107*, 3970−3980.
(39) Valásek, M.; Pecka, J.; Jindrich, J.; Calleja, G.; Craig, P. R.; Michl, J. *J. Org. Chem.* **2005**, *70*, 405−412.
(40) The scope of our discussion is mainly focused on inorganic assemblies and restricted to non-porphyrinic systems.
(41) (a) Benniston, A. C.; Harriman, A.; Li, P.; Patel, P. V.; Sams, C. A. *Phys. Chem. Chem. Phys.* **2005**, *7*, 3677−3679. (b) Benniston, A. C.; Harriman, A.; Li, P.; Sams, C. A.; Ward, M. D. *J. Am. Chem. Soc.* **2004**, *126*, 13630−13631. (c) Benniston, A. C.; Harriman, A.; Li, P.; Sams, C. A. *Phys. Chem. Chem. Phys.* **2004**, *6*, 875−877. (d) Benniston, A. C.; Harriman, A.; Li, P.; Sams, C. A. *Tetrahedron Lett.* **2003**, *44*, 4167−4169.
(42) Johansson, O.; Borgström, M.; Lomoth, R.; Palmblad, M.; Bergquist, J.; Hammarström, L.; Sun, L.; Åkermark, B. *Inorg. Chem.* **2003**, *42*, 2908−2918.
(43) Miller, S. E.; Lukas, A. S.; Marsh, E.; Bushard, P.; Wasielewski, M. R. *J. Am. Chem. Soc.* **2000**, *122*, 7802−7810, and refs. therein.
(44) (a) Ward, M. D. *Chem. Soc. Rev.* **1995**, 121−134. (b) Pierce, D. T.; Geiger, W. E. *Inorg. Chem.* **1994**, *33*, 373−381. (c) Dong, T.-Y.; Huang, C.-H.; Chang, C.-K.; Wen, Y.-S.; Lee, S.-L.; Chen, J.-A.; Yeh, W.-Y.; Yeh, A. *J. Am. Chem. Soc.* **1993**, *115*, 6357−6368. (d) Larson, S. *J. Am. Chem. Soc.* **1981**, *103*, 4034−4040. (e) Tanner, M.; Ludi, A. *Inorg. Chem.* **1981**, *20*, 2348−2350. (f) Fisher, H.; Tom, G. M.; Taube, H. *J. Am. Chem. Soc.* **1976**, *98*, 5512−5517.
(45) Tapolsky, G.; Duesing, R.; Meyer, T. J. *Inorg. Chem.* **1990**, *28*, 2285−2297.
(46) (a) Gourdon, A. *New. J. Chem.* **1992**, *16*, 953−957. (b) Woitellier, S.; Launay, J.-P.; Joachim, C. *Chem. Phys.* **1989**, *131*, 481−488. (c) Joachim, C.; Launay, J.-P. *Chem. Phys.* **1986**, *109*, 93−99.
(47) Ciofini, I.; Lainé, P. P.; Bedioui, F.; Adamo, C. *J. Am. Chem. Soc.* **2004**, *126*, 10763−10777.
(48) Busby, M.; Liard, D. J.; Motevalli, M.; Toms, H.; Vlcek, A., Jr. *Inorg. Chim. Acta* **2004**, *357*, 167−176.
(49) Liard, D. J.; Busby, M.; Farrell, I. R.; Matousek, P.; Towrie, M.; Vlcek, A., Jr. *J. Phys. Chem. A* **2004**, *108*, 556−567.
(50) Damrauer, N. H.; McCusker, J. K. *J. Phys. Chem. A* **1999**, *103*, 8440−8446.
(51) Damrauer, N. H.; Weldon, B. T.; McCusker, J. K. *J. Phys. Chem. A* **1998**, *102*, 3382−3397.

or postulated[54] for a few other inorganic compounds upon charge-transfer (CT) excitation. In the present case, torsional motions are anticipated to correlate with undesired fluctuation of the determining intercomponent electronic coupling.[47,55,56] Beyond ground state requirements, it is therefore of paramount importance to take into account possible structural changes that could occur in the excited state when engineering photoactive supramolecular architectures intended to undergo large electronic redistribution.

The present work is aimed at (i) taking advantage of appealing potentialities of triarylpyridinio-functionalized tpy ligands (Chart 1) to improve the working mode of derived PMDs and (ii) gaining new insights into the basic factors which control photoinduced processes at the intramolecular level.[35] In this study, Ru(II) complexes (**6** − **10**; Chart 2) are mainly viewed as reference compounds for the more interesting Os(II)-based analogues (**1** − **5**; Chart 2). Thus, on one hand, a further increase of conformational locking about the P−A linkage has been achieved by replacing the phenyl spacer (ph) by a *meta*-xylyl one (xy) in order to make sure that geometrical decoupling is real especially *in the excited state*. On the other hand, to improve thermodynamics of intramolecular PET between *P (the primary electron donor) and A subunits, we show here that derivatization of TP^+ by an electron-withdrawing group such as nitro (to give $TPH_2(NO_2)^+$; Chart 2) indeed results in an increased efficiency for CSS formation. These two parameters (that is xylylic modification and nitro-substitution) have been varied separately by synthesizing dyads $[(ttpy)M(tpy\text{-}xy\text{-}TPH_3^+)]^{3+}$ (**3**, **8**) and $[(ttpy)M(tpy\text{-}ph\text{-}TPH_2(NO_2)^+)]^{3+}$ (**4, 9**), respectively. Effects of these specific changes over photophysical behavior of dyads were studied by comparison with the corresponding reference $[(ttpy)M(tpy\text{-}ph\text{-}TPH_3^+)]^{3+}$ (**2**, **7**) native systems.[37] Dyads comprising both improvements, $[(ttpy)M(tpy\text{-}xy\text{-}TPH_2(NO_2)^+)]^{3+}$ (**5**, **10**), were also investigated and demonstrated to behave in a distinct manner from their parent complexes. In particular, a comparative study of **4** and **5** has allowed to assess the role of intramolecular conformation in gating intercomponent photoinduced processes like PET and electronic energy transfer (EnT).

2. Results and Discussion

2.1. Syntheses and Structural Characterization. 2.1.1. Synthesis. Triarylpyridinio-derivatized organic ligands, tpy-*sp*-TP^+ (*sp* is the phenyl or xylyl spacer), are readily available in good yields by reacting properly chosen amine precursors (tpy-*sp*-NH_2) and pyrylium salts.[37b] To obtain heteroleptic compounds (i.e., dyads), the usual synthetic route[12] consists in reacting tpy-*sp*-TP^+ with an inorganic precursor bearing a ttpy ancillary ligand ((ttpy)MCl_3) to give $[(ttpy)M(tpy\text{-}sp\text{-}TP^+)]^{3+}$.[37b] This strategy could successfully be applied for the Ru(II)-based species but not for the Os(II) analogues in the cases of the ligands bearing nitro-substituted TP^+ acceptors. Indeed, it appeared that during the last step of complexation that requires rather harsh conditions ($T \geq 383$ K and use of a reducing agent

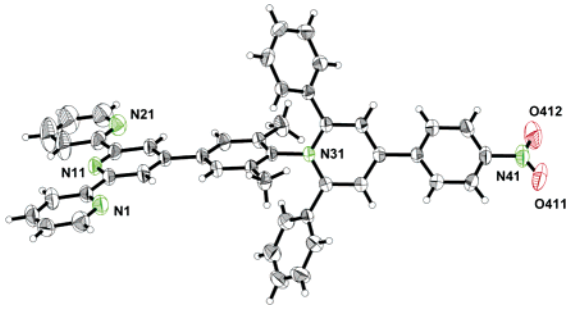

Figure 1. ORTEP drawing of the tpy-xy-$TPH_2(NO_2)^+$ ligand with thermal ellipsoids (50% probability). The BF_4^- counterion and the cocrystallized solvent molecule are omitted for clarity.

Chart 3. Relevant Angular Parameters and Nomenclature. Ph^1 Becomes Xy When R^0 = Me

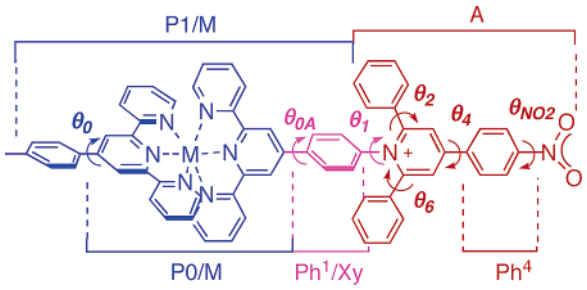

to help in labilizing chloride ligands of $(ttpy)OsCl_3$ chemically inert precursor), the tpy-*sp*-TP^+−NO_2 ligand was involved in a reductive degradation. To overcome this unexpected drawback, the so-called "chemistry-on-the-complex" approach[57−60] has been adopted. Here, this strategy consists first in building the inorganic core bearing an amino substituent at the right location (typically the photosensitizing subunit $(ttpy)M(tpy\text{-}sp\text{-}NH_2)$[59]) so that, in a second step, one is allowed to perform *in mild conditions* (that is $T \leq 350$ K) the reaction leading to the formation of the targeted nitro-derivatized triarylpyridinio fragment (Scheme SI-1b; Supporting Information). Identity of all organic models, ligands and related complexes has been confirmed by standard analytical techniques, including ^1H NMR spectroscopy, mass spectrometry and elemental analysis.

2.1.2. Structural Characterization. Ligand tpy-xy-$TPH_2(NO_2)^+$ is readily crystallized as a tetrafluoroborate salt (Figure 1) by slow evaporation of acetonitrile solution.

The main structural feature of the ligand is the dihedral angle (θ_1; Chart 3) between the planes of the *m*-xylyl spacer and pyridinium ring: 74.03°, to be compared with that of the closely affiliated tpy-ph-TPH_3^+ native ligand: 72.60°.[37b] Apparently, increased steric hindrance about the intercomponent linkage does not result in significantly larger geometrical decoupling although passing from *restrained* conformation to a more *constrained* one. This finding indicates that equilibrium conformation of the native ligand in the ground state is virtually the same as that of optimized ligand. This equilibrium geometry has been shown to change slightly upon ligand complexation, the related twist

(52) Damrauer, N. H.; Boussie, T. R.; Devenney, M.; McCusker, J. K. *J. Am. Chem. Soc.* **1997**, *119*, 8253−8268.
(53) Chen, P.; Curry, M.; Meyer, T. J. *Inorg. Chem.* **1989**, *28*, 2271−2280.
(54) Berg-Brennan, C.; Subramanian, P.; Absi, M.; Stern, C.; Hupp, J. T. *Inorg. Chem.* **1996**, *35*, 3719−3722.
(55) Cotlet, M.; Masuo, S.; Luo, G.; Hofkens, J.; Van der Auweraer, M.; Verhoeven, J.; Müllen, K.; Xie, X. S.; De Schryver, F. *Proc. Natl. Acad. Sci. U.S.A.* **2004**, *101*, 14343−14348.
(56) Weiss, E. A.; Tauber, M. J.; Kelley, R. F.; Ahrens, M. J.; Ratner, M. A.; Wasielewski, M. R. *J. Am. Chem. Soc.* **2005**, *127*, 11842−11850.
(57) Welter, S.; Salluce, N.; Benetti, A.; Rot, N.; Belser, P.; Sonar, P.; Grimsdale, A. C.; Müllen, K.; Lutz, M.; Spek, A. L.; De Cola, L. *Inorg. Chem.* **2005**, *44*, 4706−4718, and refs therein.
(58) Cooke, M. W.; Hanan, G. S.; Loiseau, F.; Campagna, S.; Watanabe, M.; Tanaka, Y. *Angew. Chem., Int. Ed.* **2005**, *44*, 4881−4884.
(59) Baranoff, E.; Dixon, I. M.; Collin, J.-P.; Sauvage, J.-P.; Ventura, B.; Flamigni, L. *Inorg. Chem.* **2004**, *43*, 3057−3066.
(60) Johansson, O.; Lotoski, J. A.; Tong, C. C.; Hanan, G. S. *Chem. Commun.* **2000**, 819−820, and refs therein.

Table 1. Electronic Absorption Data and Assignments[a]

	λ_{max} [nm] (ϵ [10^4 M^{-1} cm^{-1}])		
entry	LC	^{1}MLCT	^{3}MLCT
0	230 (4.70), 270 (5.13), 312 (8.10)	477 (1.74), 536sh (0.74)	632 (0.43), 658 (0.47)
1	286 (7.64), 314 (8.64)	490 (3.01)	645 (0.67), 668 (0.77)
2	289 (7.81), 315 (11.22)	492 (3.32)	642 (0.68), 668 (0.77)
3	290 (7.56), 315 (11.30)	491 (3.27)	642.9 (0.68), 669.2 (0.78)
4	290sh (8.34), 314 (9.86)	492 (3.07)	643.2 (0.64), 669.7 (0.72)
5	289sh (9.40), 314 (11.46)	491 (3.37)	643.2 (0.70), 670.1 (0.80)
6	285 (7.86), 310 (8.77)	490 (3.39)	
7	288 (8.62), 312 (11.65)	492 (3.63)	
8	288sh (7.91), 312.3 (10.96)	492 (3.39)	
9	289sh (9.62), 309.3 (10.64)	492 (3.34)	
10	289sh (9.28), 310.6 (11.19)	492 (3.48)	

[a] Acetonitrile solutions; sh: shoulder.

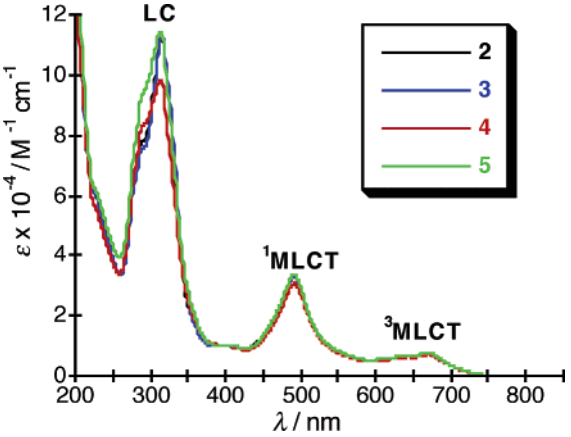

Figure 2. Electronic absorption spectra of the **2**−**5** series of Os-based compounds in solution in MeCN.

angle getting even more pronounced ($\theta_1 \approx 85.4°$ on average).[61] Thus, rather than increasing geometrical decoupling, methyl substituent of the *meta*-xylyl spacer are actually expected *to lock* the tilted conformation so as *to prevent from possible planarization* in the excited state, instead. In other words, R^0 substituents are expected to play a *structural* role mostly *in the excited state*.

2.2. Absorption Spectra. Ground-state electronic absorption spectra of reference chromophores and related inorganic dyads are collected in Table 1. Figure 2 shows the superimposed absorption spectra of **2**−**5**.

The electronic spectra of compounds **1**−**5** exhibit intense absorption bands in the UV region, due to ligand-centered (LC) transitions (ϵ in the range 10^5−10^6 M^{-1} cm^{-1}), and moderately intense absorption bands in the visible region of the spectrum, attributed to spin allowed singlet metal-to-ligand charge transfer (^{1}MLCT) transitions ($\epsilon \approx 10^5$ M^{-1} cm^{-1}). At lower energy, spin-forbidden ^{3}MLCT are also observed thanks to the presence of osmium(II) heavy metal ion. From inspection of electronic absorption properties (Table 1), it appears that the P1/M chromophore photosensitizer (Chart 3), modeled by [Os(tpy-ph-Me)$_2$]$^{2+}$ i.e., **1**, is only very scarcely affected by TP^+. Thus, ground-state electronic absorption spectra of the new dyads **3**−**5** and **8**−**10** are almost the same as those of reference native dyads **2** and **7** already published,[37b] respectively. This is indicative of a very weak electronic coupling between the P and A subunits *in the ground state*.

(61) Lainé, P. P.; Ciofini, I.; Ochsenbein, P.; Amouyal, E.; Adamo, C.; Bedioui, F. *Chem. Eur. J.* **2005**, *11*, 3711−3727.

Table 2. Electrochemical Data and Formal Assignment (See Text) of Redox Processes for Examined Model Acceptors and Complexes in Acetonitrile + 0.1 M $TBABF_4$ at Pt Electrode[a]

	$M^{III/II}$		$TP^{+/0}$		$TP^{0/-}$		$P^{0/-}$		$P^{-/2-}$	
entry	$E_{1/2}$	n	$E_{1/2}$	n	$E_{1/2}$	n	$E_{1/2}$	n	$E_{1/2}$	n
ph-TPH_3^{+}[b]			−0.93	1	−1.08	1				
xy-TPH_3^{+}			−0.98	1	*c*					
ph-$TPH_2(NO_2)^{+}$			−0.70[d]	1[d]	−0.70[d]	1[d]				
xy-$TPH_2(NO_2)^{+}$			−0.66	1	−0.81	1				
0	+0.95	1					-1.16_5	1	−1.45	1
1[b]	+0.90	1					−1.20	1	−1.47	1
2[b]	+0.93	1	−0.91	1[e]	−1.00	1[e]	−1.21	1	−1.47	1
3	+0.95	1	−0.93	1	*c*		−1.17	1	−1.46	1
4	+0.93	1	−0.65[f]	1	−0.74[f]	1	−1.21[g]	nd	−1.47[g]	nd
5	+0.93	1	−0.63	1	−0.79	1	−1.17	1	−1.45	1
6[b]	+1.24	1					−1.24	1	−1.47	1
7[b]	+1.27	1	−0.90	1	−1.00	1	−1.25	1	−1.50	1
8	+1.27	1	−0.94	1	*c*		−1.22	1	−1.48	1
9	+1.27	1	−0.66[f]	1	−0.73[f]	1	−1.24[g]	nd	−1.51[g]	nd
10	+1.27	1	−0.63	1	−0.78	1	−1.20	1	−1.46	1

[a] $E_{1/2}$/V (vs SCE) is calculated as (E_{pa} + E_{pc})/2 where E_{pa} and E_{pc} are the anodic and cathodic peak potentials measured by cyclic voltammetry at 0.2 V s^{-1} ; n is the number of electrons involved in the redox process determined by hydrodynamic voltammetry by comparison with reference components or with respect to the internal monoelectronic oxidation of the metal center for complexes; nd: not determined. [b] ref 37a. [c] Out of the investigated potential window (below −1.70 V). [d] Two unresolved monoelectronic processes corresponding to $TP^{+/0}$ and $TP^{0/-}$ observed as a bielectronic peak. [e] Two monoelectronic partially resolved peaks: $TP^{+/0}$ cathodic peak merges with $TP^{0/-}$. [f] ill-resolved peaks. [g] Reported value refers to E_{pc} and ill-defined reversible process due to electrode surface modification upon potential scanning below −1.1 V.

2.3. Redox Behavior. The electrochemical properties of model organic acceptors, reference complex-photosensitizers and dyad systems are gathered in Table 2, where Ru(II) complexes data are also included for comparison.

Assignment of redox processes within the various dyads investigated has been made on the basis of issues obtained from the electrochemical study of model parent species. The following picture can be drawn out of these electrochemical data:

(i). In the ph-TPH_3^+ model acceptor (Chart 2) and in the corresponding metal complexes **2** and **7**, the TP^+ subunit is doubly reduced at mild potentials (ca., −1 V; Table 2**)**. The difference in potential between the two TPH_3^+-based reduction processes is relatively small (150 mV for the isolated parent acceptor and equals 90 and 100 mV for the osmium and ruthenium complexes, respectively), so indicating a large delocalization of the redox-active orbital, which is probably extended over many of the rings.

(ii). When comparing various TPH_3^+-based species (Chart 2, Table 2, Figure 3a), it appears that when θ_1 is conforma-

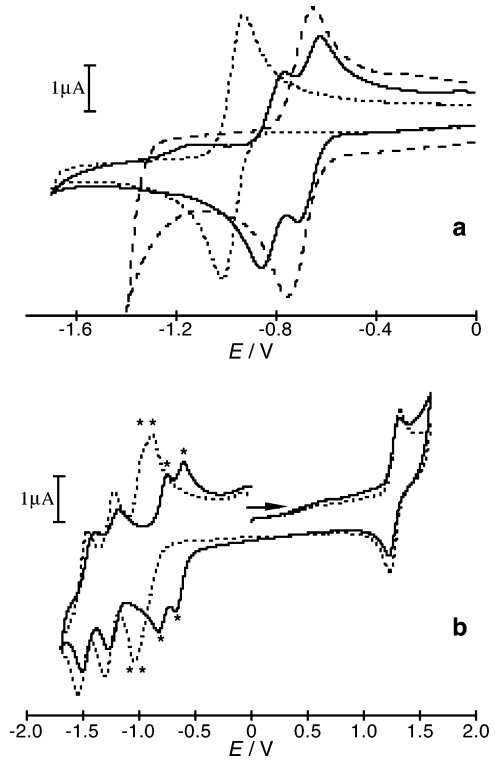

Figure 3. (a) Cyclic voltammograms ($v = 0.2$ V s^{-1}) for *xy*-TPH_3^+ ($c = 5.5 \times 10^{-4}$ M; dotted line), ph-$TPH_2(NO_2)^+$ ($c = 3.1 \times 10^{-4}$ M; dashed line) and *xy*-$TPH_2(NO_2)^+$ ($c = 3.3 \times 10^{-4}$ M; solid line). (b) Cyclic voltammograms for **6** ($c = 2.4 \times 10^{-4}$ M, $v = 0.3$ V s^{-1}; dotted line)[37a] and **10** ($c = 1.4 \times 10^{-4}$ M, $v = 0.2$ V s^{-1}; solid line). The * indicates redox processes related to the acceptor unit.

tionally *constrained*, as in the case of *xy*-TPH_3^+, the second reduction of the acceptor is displaced to much more negative potentials, out of the investigated (and accessible) potential window. In the case of rings for which rotation around θ_1 is only *restrained* (e.g., ph-TPH_3^+), once the pyridinium has gained one electron, the three-ring segment (comprising the *N*-phenyl group (Ph^1), the pyridinium ring (Py^+) and terminal phenyl moiety (Ph^4); Chart 3), can adopt a more planar conformation as a result of a quinoid-like electronic redistribution of the reduced pyridinium. Such a propensity for *planarization* is expected to get even more pronounced upon second reduction, i.e., on going from radical to monoanion, as the second gained electron is anticipated to be delocalized over the whole segment[38] instead of being preferably "localized" on the heterocycle.[62] Upon limiting (i.e., constraining and even locking) torsional motion about θ_1 (case of *xy*-TPH_3^+), the latter supplementary planarization is hindered so that the second reduction is found to be energetically unfeasible under standard conditions.

(iii). Addition of a nitro substituent onto TP^+ at the R^2 position does result in a substantial increase of the electron-withdrawing capability of this latter, as expected. Indeed, a positive potential shift of ca. +0.25 V of the redox processes is clearly observed (Table 2), which well compare with redox behavior of a series of 4-[substituted-phenyl]-pyridinium species reported in the literature.[63] Interestingly, possibility of double reduction of the acceptor is restored upon nitro-derivatization in the case of conformationally locked *xy*-$TPH_2(NO_2)^+$ model and related dyads **5** and **10**. Thus, the main, chemical, contribution to redox active orbital is apparently shifted from the [Ph^1/Xy-Py^+] system toward the [Py^+−Ph^4−NO_2] terminal one. It remains nonetheless that the model acceptor, when on the whole a monoanion species, is somewhat energetically less favored in the case of [*xy*-$TPH_2(NO_2)]^-$ due to constrained rotation about θ_1 ($E = -0.81$ V) than in [ph-$TPH_2(NO_2)]^-$ ($E \approx -0.70$).[53] This point, together with the fact that $TPH_2(NO_2)^+$ could only be *doubly* reduced (like unlocked native acceptor unit) but not three times reduced, as would be expected for a nitrophenyl moiety decoupled from the pyridinium core, further confirms the relevance of the *delocalized description of the pyridinium-centered A component comprising the N-pyridinio aryl substituent (Ph^1 or Xy) and the Ph^4-NO_2 group*.

(iv). The comparison of ph-TPH_3^+ to *xy*-TPH_3^+ and of ph-$TPH_2(NO_2)^+$ to *xy*-$TPH_2(NO_2)^+$ data definitively indicates that the reduction pattern of the pyridinium core is not only sensitive to the *nature* of attached *N*-pyridinio substituent, as shown in previous works,[37,61] but also to the *tilt angle* θ_1. More precisely, the TP^+ fragment is found to be two-times reducible *at the most* under favorable conditions including *allowed planarization about θ_1 and/or derivatization with conjugated and strongly electron-withdrawing substituents* such as NO_2.

(v). The redox processes related to the photosensitizer unit (metal- and terpyridyl ligands- centered) within the various new dyads are almost unaffected by the modification of neither the acceptor moiety nor the spacer (with respect to native dyads, **2** and **6** Chart 2; Figure 3b). Moreover, it is noteworthy that, although bielectronically reduced, $[TP]^-$ does not influence a lot the subsequent (ph-)tpy-centered reduction process referred to as $P^{0/-}$ (Table 2). Taken together, these findings demonstrate the weak intercomponent electrostatic interaction (and electronic coupling) *in the ground state*.

2.4. Spectroelectrochemical Behavior. To facilitate the interpretation of the transient absorption spectra and more particularly to identify the formation of charge-separated states where the photosensitizer is oxidized (metal-centered process), while the acceptor unit is reduced, three spectroelectrochemical experiments have been undertaken. On one hand, the gradual reduction of the model acceptor *xy*-$TPH_2(NO_2)^+$ has been performed, up to add two electrons per molecule (i.e., successive formation of the singly and doubly reduced species *xy*-$TPH_2(NO_2)^0$ and xy-$TPH_2(NO_2)^-$, respectively). On the other hand, the controlled monoelectronic oxidation of the osmium- and ruthenium-based optimized dyads (**5** and **10**, respectively) was performed in order to get the spectroscopic signature of the embedded P1/M photosensitizers when oxidized (Supporting Information: Figure SI-2a−c).

The reduced model acceptor as well as the oxidized photosensitizers within $[\mathbf{5}]^+$ and $[\mathbf{10}]^+$ are good chromophores as they exhibit new absorption bands with extinction coefficient larger than 10 000 M^{-1} cm^{-1}. Unfortunately, the main spectroscopic signatures of $[A]^-$ and $[P]^+$ are found to be intermingled in the of 400 − 500 nm spectral region, as already noticed for **2**,[37,47] making it difficult to interpret transient absorption difference spectra of photoexcited dyads.[47,64] Actually, the more diagnostic

(62) Bock, H.; Herrmann, H.-F. *Helv. Chim. Acta* **1989**, *72*, 1171−1185.
(63) Hasegawa, E.; Kang, D.; Sakamoto, K.; Mitsumoto, A.; Nagano, T.; Minakami, S.; Takeshige, K. *Arch. Biochem. Biophys.* **1997**, *337*, 69−74.
(64) Noteworthy, the broad features situated at 400−500 nm also overlap absorption of nitrobenzene radical anion if formed, which occurs at ca. 455 nm in DMF (Miertus, S.; Kysel, O.; Danciger, J. *Collect. Czech. Chem. Commun.* **1980**, *45*, 360−368).

Table 3. Absorption Maxima of the Electrochemically Reduced and Oxidized Key Species[a]

entry	λ_{max} [nm] (ϵ [10^4 M^{-1} cm^{-1}])			
xy-$TPH_2(NO_2)^0$ (i.e., A_{ref} + 1e-)	440 (2.28)	471 (2.70)	830 sh(0.83)	>900 (>1.50)
xy-$TPH_2(NO_2)^-$ (i.e., A_{ref} + 2e-)	474 (2.45)	526 (2.33)		
[5]$^+$	404 (2.80)	517 (0.64)	608 (0.37)	
[10]$^+$	375 sh (2.55)		690 (0.35)	

[a] As the singly and doubly reduced model acceptor cannot be obtained in pure forms (due to the close potential values of the two successive redox processes related to the reduction of the pyridinium) the given value for the respective extinction coefficients of their characteristic absorption bands are only estimates.

Table 4. Photophysical Data for the Various Dyads and Reference Photosensitizers

	293 K[a]				77 K[b]	
entry	λ_{max} [nm]	Φ_{em} ($\times 10^2$)	I_{em}rel [%][c]	τ [ns]	λ_{max} [nm]	τ [μs]
0	724	1.40	70	269	689	3.9
1[d]	736.5	2.00	100	247	721, 790sh	3.1
2[d]	751	1.02	50.9	168	726, 790sh	2.7
3	749	1.23	61.7	191	728, 790sh	3.2
4	745	0.092	4.6	174	725, 790sh	3.1
5	743.5	0.0318	1.6	<10	729, 790sh	3.2
6	640	0.0032		0.58[d]	627, 684sh[d]	11.7[d]
9	676	0.011		7	645, 696sh	10.0
10	674	0.009		1	637, 685sh	12.5

[a] In acetonitrile. [b] In butyronitrile. sh: shoulder. [c] I_{em}rel = 100 × [Φ_{em}(species)/Φ_{em}(**1**)]. [d] ref 37a.

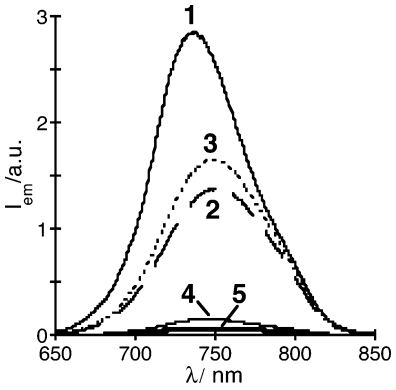

Figure 4. Emission spectra of the Os(II) series of complexes in deaerated MeCN solutions at room temperature, measured in identical experimental conditions (in particular, same OD at $\lambda_{exc.}$ = 600 nm).

region appears to be situated at λ > 710 nm and in particular in the NIR domain (around 900 nm) where the mono-reduced acceptor only (that is *xy*-$TPH_2(NO_2)^0$) exhibits a significant absorption (Table 3).

2.5. Photophysical Behavior. 2.5.1. Luminescence Properties. All the Os(II) species investigated here are luminescent, both in acetonitrile fluid solution at room temperature (rt) and in butyronitrile rigid matrix at low temperature (lt), i.e., 77 K (see Table 4). In all cases, emission can be straightforwardly attributed to the lowest lying ^{3}MLCT state of the photosensitizer.

When compared to complex **1**, complexes **2**−**5** all exhibit reduced luminescence quantum yields (Figure 4) and lifetimes at room temperature. From the analysis of the photophysical data, it appears that, as far *as the emission energy is concerned*, the main perturbation of the luminescent ^{3}MLCT state in this series of complexes results from the covalent appending of the positively charged triarylpyridinium (TP^+) group to P1/Os luminophore (by taking **1** and **6**, for the analogous Ru(II) species, as references). Indeed, emission of complexes **2**−**5** is red-shifted compared to that of **1**, most likely because the TP^+-derivatized aryl-tpy ligand is made easier to reduce than the nonsubstituted one, so decreasing the MLCT excited-state energy.[65] Other additional modifications concerning either the photosensitizer itself (i.e., the methyl substituents of the xylyl moiety, as in **3**) or the acceptor group (i.e., NO_2, as in **4**) or both (as in **5**) are actually found to barely influence the emitting level of the luminophore, which roughly lies at the same energy throughout the **2**−**5** series. This fact is illustrated in normalized rt and 77 K emission spectra of the whole series of complexes (Figures SI-3a and b; Supporting Information). These findings are not surprising for the following reasons. First, even if methyl groups of the xylyl spacer (in **3** and **5**) are weak electron-donating substituents (+*I* effect), inductive contribution is known to be a short-range effect. Second, although NO_2 substituent exerts pronounced π-extending (-*M* mesomeric effect) and inductive electron-withdrawing (-*I* effect) influences over the terminal phenyl of TP^+ and linked pyridinium ring within **4** (and **5**), these effects are anticipated to hardly propagate to the metal center, over ca. 18 Å and through 16/17 covalent bonds. Indeed, the π-system is not fully delocalized due to cumulated structural distortions along the main molecular axis, especially about the canted pyridinium (θ_1) (Chart 3).

Table 5. Excited-State Properties of the Various Dyads and Reference Photosensitizers[a]

entry	E(III/II*)[V]	E(II*/I)[V]	ΔG_{ET}[eV]	k_r [s^{-1}]	k_{nr} [s^{-1}]
1	−0.820	+0.520		8.1×10^4	4.0×10^6
2	−0.778	+0.498	+0.132	6.1×10^4	5.9×10^6
3	−0.753	+0.533	+0.177	6.4×10^4	5.2×10^6
4	−0.780	+0.495	−0.125	5.3×10^3	5.7×10^6
5	−0.771	+0.531	−0.141	$>3.2 \times 10^4$	$>9.9 \times 10^7$
6	−0.737	+0.737		5.5×10^4	1.7×10^9
9	−0.652	+0.682	+0.0075	1.6×10^4	1.4×10^8
10	−0.676	+0.746	−0.046	9.0×10^4	9.9×10^8

[a] Excited-state redox potentials E(III/II*) and E(II*/I) as well as radiative (k_r) and nonradiative (k_{nr}) rate constants were calculated according to refs 71 and 72.

The luminescence data of **1**−**3** suggest that oxidative electron transfer from the MLCT chromophore to the TP^+ acceptor is not effective. In fact, the driving force of the process is almost negligible or even endoergonic (Table 5), making electron-transfer inefficient. As far as species **2** and **3** are concerned,

(65) Noticed differential sensitivity of P1/Os electronic features to TP^+ attachment depending on whether electronic absorption or emission properties are considered is indicative of differences stemming from the actual nature of both involved P/A partners and their electronic interplay. Indeed, greater sensitivity of emission properties (Table 4) as compared to that of absorption properties (Table 1) is most likely related to the (ML)-CT nature of the intramolecular probe directly linked to the TP^+ group, which is [(ttpy)Os^{3+}(tpy-ph)$^-$] in the former case versus [(ttpy)Os^{2+}(tpy-ph)] in the latter one. In the present case, ground state picture derived from methods like electronic absorption and electrochemistry cannot be straightforwardly extrapolated to excited state. This finding is a consequence of existing nonnegligible intercomponent electronic coupling and is not observed when electronic insulation is strictly attained, as in the case of methylene linked assemblies; see ref 66.

the above cited luminescence properties difference can *now*[67] be essentially attributed to the energy gap law.[68] The fact that **3** is slightly more emissive than **2** can be ascribed to increased rigidity of the supermolecule architecture[69] and is more specifically indicative of the efficacy of R^0 methyl groups in constraining conformational fluctuations *in the excited state*,[70] as expected. Thus, **3** and **2** are now worth considered as new references (for P1/Os luminophore with locked and unlocked chromophoric ligand, respectively) rather than **1**[2a] for forthcoming photophysical study of photoinduced processes within dyads **5** and **4**, respectively.

Energy gap law alone cannot justify the significant reduction in luminescence quantum yields and lifetimes of **5** and -to a smaller extent- **4** (Table 4 and Figure 4). Therefore, at least another decay channel has to be active in these species. At 77 K, the luminescence properties of all the species are quite similar one another (Table 4), suggesting that the supplementary decay channel operating in **4** and **5** at room temperature is not active at lt, in rigid matrix.

When comparing the estimated excited-state reducing strength of the metal chromophore in *[**5**] (E(III/II*) = −0.77 V) to the first reduction potential of the acceptor TP^+ (i.e., $E((NO_2)H_2TP^{+/0})$ = −0.63 V), it appears that an oxidative quenching of the excited photosensitizer (primary light-triggered donor) by the TP^+ subunit is thermodynamically allowed by ca. $\Delta G = -0.140$ eV. Similar exoergonicity of ca. −0.125 eV is found for **4**. One can note that the driving force for an intramolecular PET is only very slightly favorable in the case of the ruthenium analogue of **5**, that is **10**. Therefore, the reduction in luminescence lifetimes (for **5**) and quantum yields (for both **4** and **5**) could in principle be attributed to the occurrence of a photoinduced intramolecular ET (oxidative quenching of *P). Obviously, because of the small driving force, this process is expected to be inefficient in rigid matrix at 77 K, and this would explain the low-temperature emission properties. Indeed, due to precluded solvent repolarization on the time scale of the excited-state lifetime, electronic redistribution that accompanies PET process is estimated to require ca. +0.6 eV to take place.[73,74] In the present case, such a contribution makes the slightly exoergonic reactions at room temperature largely endoergonic at 77 K. However, reduction in emission quantum yield at room temperature is not accompanied by a reduction in phosphorescence lifetime in **4**, suggesting that the hypothesis of a simple ET quenching does not hold, at least for this latter species.

It should be noted that when dealing with excited-state energy of the ^{3}MLCT state, which is relevant for the calculation of the electron-transfer driving force, the following particular point should be considered. Although **4** and **5** (as well as **2** and **3**) adopt the same -more stable- axially distorted geometry resulting from intraligand steric hindrance (especially about θ_1; Chart 3) in the ground state, the question arises of whether experimentally derived $E_{em}(0-0)$ values actually correspond to dyads in their tilted (frozen ground state) conformation or in their *planarized geometry* (see below: section **2.5.2A**). In the former case, emission spectra recorded at low temperature (in *rigid* matrix) afford $E_{em}(0-0)$ values related to the room temperature *not relaxed* (*NR*) ^{3}MLCT state of P1/Os, which is different from the room temperature -thermalized (i.e., *relaxed*, *R*)- planar ^{3}MLCT *emitting* state. Emission maxima measured at 77 K are therefore worth referred to as $E_{em}(0-0)_{NR}$ (where index "NR" also identifies the "tilted conformation") and $E_{em}(0-0)_R$, respectively. Indeed, it is anticipated that $E_{em}(0-0)_{NR} > E_{em}(0-0)_R$ due to extended electronic delocalization over the whole planarized aryl-tpy ligand.[75]

Interestingly, it has been stated in the related case of *N*-methyl-4,4′-bipyridinium (MQ^+) acceptor that although the planarization mode could be inhibited in the rigid glass,[53] it appears not to be in the complex $[(4,4'\text{-}(NH_2)_2bpy)Re(CO)_3(MQ^+)]^{2+}$. In this complex, emission from the equilibrated $d\pi \rightarrow \pi^*$ (MQ^+) state is observed in the glassy state at low temperature.[76] Also, it has been estimated a rather large thermodynamic driving force of ca. 7 kcal mol^{-1} (i.e., 29 kJ mol^{-1} or 0.3 eV) for achieving the planarization of reduced phenyl-bpy (that models the ligand when involved in the (ML)-CT state of related complex).[52] On the basis of the latter energetic estimate for planarization, the assumption that experimentally measured value for $E_{em}(0-0)$ is actually related to $E_{em}(0-0)_{NR}$ rather than $E_{em}(0-0)_R$ would mean that PET processes (i.e., CS formations) within **4** and **5** are not slightly *exoergonic* (by ca. −0.125 eV and −0.141 eV for **4** and **5**, respectively) but slightly *endoergonic* (by ca. +0.175 eV and +0.159 eV, respectively). Clearly, such an inference is not consistent with experimental issues herein reported, therefore, we would tentatively state that there is room for the phenyl ring of the aryl-tpy ligand to rotate in the rigid glass,[77] correlatively implying that experimentally derived value for $E_{em}(0-0)$ actually corresponds to $E_{em}(0-0)_R$.

2.5.2. Ultrafast Transient Absorption Spectroscopy. To better characterize and clarify the excited-state properties of the new osmium complexes, we performed ultrafast (fs time range) transient absorption (TA) spectroscopy in acetonitrile at room temperature. For all the osmium compounds, differential absorption spectra after laser pulse ($\lambda_{exc.}$ = 400 nm; first observation

(66) Collin, J.-P.; Guillerez, S.; Sauvage, J.-P.; Barigelletti, F.; De Cola, L.; Flamigni, L.; Balzani, V. *Inorg. Chem.* **1992**, *31*, 4112−4117.
(67) Hitherto, the status of native dyad **2** with respect to CSS formation has remained somewhat unclear.[37, 47] In particular, we could not get clear-cut picture on the reason for the decrease of emission quantum yield of P1/Os luminophore within **2**: (i) Energy gap law, due to electronic perturbation of P1/Os by appending of TP^+, for which there is no *simple* equation to quantify *a priori* the contribution (i.e., without available experimental data for a series of affiliated compounds; Anderson, P. A.; Keene, F. R.; Meyer, T. J.; Moss, J. A.; Strouse, G. F.; Treadway, J. A. *J. Chem. Soc., Dalton Trans.* **2002**, 3820−3831 and refs therein) and/or (ii) Poor efficiency of the P^+-A^- state (CS state) population from the emitting ^{3}MLCT level (PET process) moreover leading to negligible spectral changes.[47] This complexity is further increased by potentially misleading effects of intercomponent electronic coupling, as discussed in ref 47. Actually, in borderline cases like **2**, only comparison with closely affiliated species unambiguously demonstrated to undergo PET process with CSS formation can definitely help to decide. The present study provides such reference-dyads (cf. cases of **4** and **5**).
(68) Claude, J. P.; Meyer, T. J. *J. Phys. Chem.* **1995**, *99*, 51−54.
(69) Nijegorodov, N. I.; Downey, W. S. *J. Phys. Chem.* **1994**, *98*, 5639−5643 and references therein.
(70) (a) McFarland, S. A.; Finney, N. S. *J. Am. Chem. Soc.* **2002**, *124*, 1178−1179. (b) McFarland, S. A.; Finney, N. S. *J. Am. Chem. Soc.* **2001**, *123*, 1260−1261.
(71) Calvert, J. M.; Caspar, J. V.; Binstead, R. A.; Westmoreland, T. D.; Meyer, T. J. *J. Am. Chem. Soc.* **1982**, *104*, 6620−6627.
(72) Juris, A.; Balzani, V.; Barigelletti, F.; Campagna, S.; Belser, P.; Von Zelewsky, A. *Coord. Chem. Rev.* **1988**, *84*, 85−277.
(73) Amoroso, A J.; Das, A.; McCleverty, J. A.; Ward, M. D.; Barigelletti, F.; Flamigni, L. *Inorg. Chim. Acta* **1994**, *226*, 171−177.
(74) Gaines, G. L.; III.; O'Neil, M. P.; Svec, W. A.; Niemczyk, M. P.; Wasielewski, M. R. *J. Am. Chem. Soc.* **1991**, *113*, 719−721.
(75) Strouse, G. F.; Schoonover, J. R.; Duesing, R.; Boyde, S.; Jones, W. E., Jr.; Meyer, T. J. *Inorg. Chem.* **1995**, *34*, 473−487.
(76) Chen, P.; Danielson, E.; Meyer, T. J. *J. Phys. Chem.* **1988**, *92*, 3708−3711.
(77) Barich, D. H.; Pugmire, R. J.; Grant, D. M.; Iuliucci, R. J. *J. Phys. Chem. A* **2001**, *105*, 6780−6784.

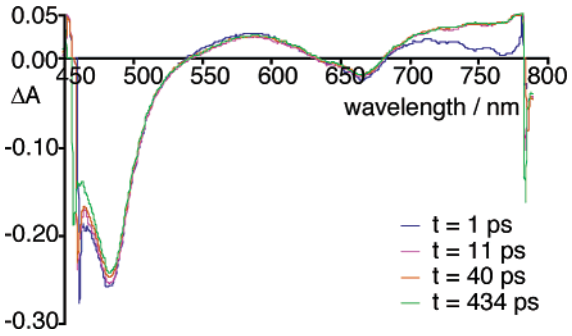

Figure 5. Selected ultrafast differential transient absorption spectra of **3**.

Table 6. Ultrafast Data with Attribution

complexes	aryl-tpy planarization process	electron transfer (or equilibration)	longer excited-state lifetime
1	2 ps		>1ns
2	5 ps		>1ns
3	2 ps		>1ns
4	2 ps	400 ps	>1ns
5	2 ps	870 ps	870 ps
6	2 ps		580 ps

after 500 fs from pulse) show a strong bleach at about 490 nm and a weaker bleach at 680 nm, which can be assigned to the expected bleaching of the spin-allowed and spin-forbidden MLCT absorption bands, respectively.[12] Transient absorption taking place in both the range of 550−630 nm and at wavelengths longer than 700 nm, is mainly ascribed to absorption of the radical anion of ligand(s).[12]

A. Excited-State Behavior of Compounds 1−3 at Room Temperature in Fluid Solution. The shape of the differential absorption spectra clearly changes in the region around 740 nm for all the species (**1**−**5**). In particular, there is a rise of the absorption accompanied by a change in the band maximum, in a time scale of a few picoseconds (Figure 5, Table 6). After this process, the transient spectra of **1**−**3** remain roughly constant (on the ps time scale), in agreement with the luminescence lifetimes (Table 4). The change of the transient absorption in the 740 nm region can be attributed to a modification in the structure of the radical anion: a similar effect has been indeed reported for $[Ru(dpb)_3]^{2+}$ (dpb = 4,4′-diphenyl-2,2′-bipyridine) and was attributed to the planarization of the two phenyl rings with respect to the bpy framework (the phenyl rings are canted with respect to bpy in the ground state and as a consequence in the initially prepared Franck−Condon excited state).[52,78] An analogous change in structure is believed to occur upon reduction of biphenyl[79,80] and dimethyl-viologen.[75] Also, such a structural relaxation toward planarity, resulting from a CT state, has been evidenced for the *N*-methyl-4,4′-bipyridinium ligand (MQ^+) within $[Re(MQ^+)(CO)_3(4,4'\text{-}Me_2bpy)]^{2+}$.[48,49,53] Time scale for the planarization of the phenyl rings in the Ru(II) complex mentioned above was of a few ps, the same time scale in which the fast process takes place in **1**−**3**. On the basis of literature data, we assign the picosecond process to *planarization* of the aryl rings directly linked to the tpy ligands (θ_0 and $\theta_{0A} \rightarrow 0$; Chart 3).

A further argument supporting our assignment is the red shift of the room temperature emission energy of **1** (Table 4) compared to that of $[Os(tpy)_2]^{2+}$ (i.e., **0**, λ_{max} = 724 nm), which implies an extended delocalization of the electron within the ligand framework in the emitting ^{3}MLCT state, once more similar to that reported for the $[Ru(dpb)_2]^{2+}$ complex.[50−52] To further test our hypothesis, we also performed the same TA experiment on $[Ru(ttpy)_2]^{2+}$ (**6**), analogous to **1**, and we found the same process occurring with the lifetime of 2 ps (cf. Figure SI-5; Supporting Information), so definitely also showing that this process does not directly involve metal orbitals.

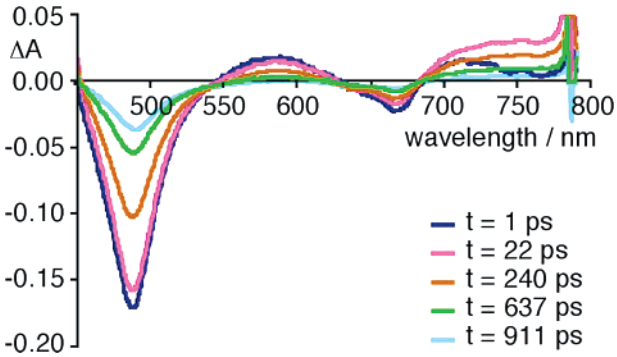

Figure 6. Selected ultrafast differential transient absorption spectra of **5**.

Interestingly, Maestri et al., within the framework of an early thorough analysis of substituents electronic effects upon the photophysical properties of the $*[Ru(tpy)_2]^{2+}$ luminophore,[81] have suspected some excited-state structural relaxation when substituent is a phenyl (analogous of **6**), even if planarization is not explicitly stated. Of note, however, more recently performed subnanosecond time scale photophysical investigations on $[Ru(ttpy)_2]^{2+}$ (**6**) and related dinuclear compounds did not allow the authors to suspect the occurrence of such a planarization although they studied the delocalization of MLCT excited states.[82] Actually, the differential transient absorption spectrum they reported[82] for **6** (taken at the end of a 35 ps pulse) closely resembles to the one recorded here for similar delay, but their temporal resolution was not sufficient to observe ultrafast (2 ps) spectral evolution.

The constancy (and the similitude) of the profile of the differential transient absorption spectra after 20 ps for complexes **1**−**3** confirms the conclusions inferred from luminescence properties as far as the inefficiency of ET quenching by the TP^+ subunit is concerned.

B. Excited-State Behavior of Dyads 4 and 5 at Room Temperature in Fluid Solution. At rt, differential transient absorption spectra of complexes **4** and **5**, after the fast ps-scale processes, exhibit a different behavior compared to those of the other osmium species (**1**−**3**). Again in this case, the more diagnostic spectral region is that at λ > 700 nm. Compound **5** transient spectrum decays to the ground state, without any significant modification in the spectral profile (apart from those related to the above-mentioned planarization process), with a single lifetime of about 900 ps (Table 6, Figure 6 and Figure SI-6 in Supporting Information). For **4**, the transient absorption

(78) McCusker, J. K. *Acc. Chem. Res.* **2003**, *36*, 876−887.
(79) Almenningen, A.: Bastiansen, O.; Fernholt, L.; Cyvin, B. N.; Cyvin, S. J.; Samdal, S. *J. Mol. Struct.* **1985**, *128*, 59−76.
(80) Furuya, K.; Torii, H.; Furukawa, Y.; Tasumi, M. *THEOCHEM* **1998**, *424*, 225−235.
(81) Maestri, M.; Armaroli, N.; Balzani, V.; Constable, E. C.; Cargill Thompson, A. M. W. *Inorg. Chem.* **1995**, *34*, 2759−2767.
(82) Hammarström, L.; Barigelletti, F.; Flamigni, L.; Indelli, M. T.; Armaroli, N.; Calogero, G.; Guardigli, M.; Sour, A.; Collin, J.-P.; Sauvage, J.-P. *J. Phys. Chem. A* **1997**, *101*, 9061−9069.

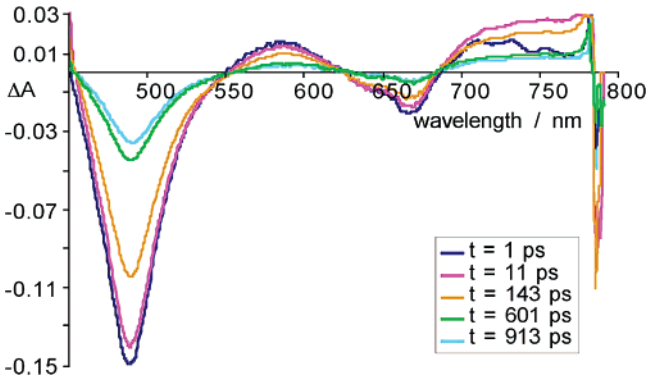

Figure 7. Selected ultrafast differential transient absorption spectra of **4**.

spectrum (Figure 7) also does not present significant differences in shape, but its decay (Figure SI-7 in Supporting Information) from the "planarized" CT state is biphasic, exhibiting an initial lifetime of 400 ps. Then, the whole transient spectrum remains approximately constant in the experimental time scale (1 ns), in agreement with the relatively long lifetime (174 ns) of the emitting state (Table 4). For more details, refer to the Experimental Section and Supporting Information.

To rationalize the behavior of **4** and **5**, let us start from our hypothesis of an oxidative ET from the ^{3}MLCT state to the TP^+-NO_2 unit. We indeed tentatively attribute the short lifetime of the excited state of **5** (870 ps from transient absorption data, < 10 ns from luminescence properties) to the occurrence of an intercomponent ET process. Rate constant of this process (taking as unquenched reference the luminescence lifetime of **3**) would be 1.1×10^9 s^{-1}. The (very short-lived and less efficient) emission would therefore be due to the quenched ^{3}MLCT state. However, formation of the charge-separated state (CSS) is not directly visible in transient absorption spectroscopy, suggesting that deactivation of the CSS to the ground state (i.e., the charge recombination process, CR) is much faster than the forward process. In other words, reduced acceptor does not accumulate, as is the case for the Os(tpy)-based triad $*[D^+$-P1-$A^-]$ (with P1 = Os(II)-bis-ttpy, A = methyl viologen and D = di-*p*-anisylamine) reported by Sauvage et al.[66] Possible contributions to this fast deactivation process could come from radiationless pathways involving the nitro group: indeed it is known that the NO_2 group induces very fast radiationless decay of MLCT levels in metal polypyridine complexes (compare the luminescence lifetimes at room temperature in aqueous solution of $[Ru(bpy)_2$(5-nitro-1,10-phenanthroline)$]^{2+}$ and $[Ru(bpy)_2$(1,10-phenanthroline)$]^{2+}$, ≤7 ns and 684 ns, respectively),[72] most likely via solvent-assisted processes.[83] Similar processes could also accelerate CR in **5**.

The situation appears more complicated for **4**. For this species, a priori and on thermodynamic basis, the transient decay of 400 ps (which translates into a quenching rate constant of 2.5×10^9 s^{-1}) could still be attributed to electron transfer, but this decay process does not lead to the ground state, which is reached on quite a longer time scale, in agreement with the luminescence lifetime (Table 4).

To understand the properties of **4**, it's worth taking into account the recently obtained results of a theoretical investigation based on Density Functional Theory (DFT).[84] This study

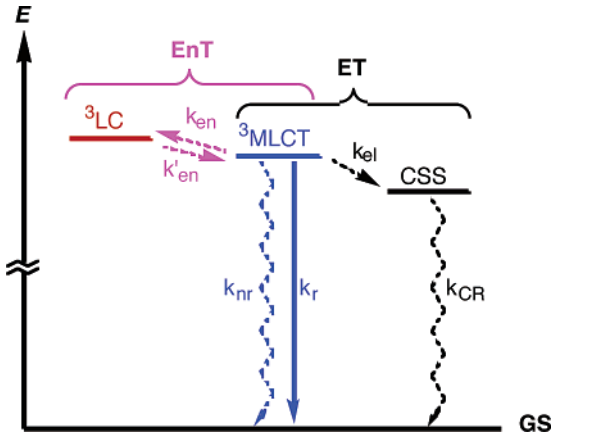

Figure 8. Schematized energy level diagram of **4** and **5**. Dashed lines and solid lines represent nonradiative and radiative processes, respectively. In **4**, k_{en} competes with k_{el} and the rate constant of the equilibration process, k_{eq} is $(k_{en} + k'_{en})$. In **5**, $k_{el} \gg k_{en}$.

is evidencing that, for both **4** and **5**, another triplet state is lying close in energy to the lowest ^{3}MLCT level. Such a state has been computed as a ligand centered (LC) state largely involving the nitro group. Supporting the theoretical issues, 77 K millisecond phosphorescence of the two A_{ref} organic acceptor models, ph-$TPH_2(NO_2)^+$ and xy-$TPH_2(NO_2)^+$ (Chart 2), has been found at about 725 nm, that is very close to the 77 K ^{3}MLCT emission of **4** and **5** (Table 4).[84] In both **4** and **5**, therefore, energy transfer (EnT) from the lowest-lying ^{3}MLCT state to such a LC (nitro-based) level[85−90] can a priori compete with the ET producing the CSS at room temperature, at least as the primary deactivation process (see Figure 8). Whether ET or EnT dominates is a matter of balance between thermodynamics and electronic coupling of the active sites. Apparently, ET is the dominant primary deactivation process for **5**, while this is not the case for **4**. For this latter species, EnT is assumed to dominate the decay from the ^{3}MLCT state, and this can lead to *equilibration* between the two triplet states, when suitable kinetic and thermodynamic parameters are fitted.[91] The equilibrated ^{3}MLCT state level can then (i) undergo ET to form the targeted CSS, which rapidly decays back to the ground state (CR), as for **5** or (ii) directly deactivate to the ground state. Both of the hypotheses justify the reduced quantum yield of **4** in comparison with that of **1**, as well as its relatively long luminescence lifetime (174 ns). In both cases, we tentatively assign the 400 ps decay obtained by transient spectroscopy to the equilibration time while the luminescence lifetime can be ascribed (i) to the quenched lifetime of the equilibrated state, whose *unquenched* intrinsic

(83) Gabrielsson, A.; Matousek, P.; Towrie, M.; Hartl, F.; Zalis, S.; Vlcek, A., Jr. *J. Phys. Chem. A* **2005**, *109*, 6147−6153.

(84) Part 2: Lainé, P. P.; Loiseau, F.; Campagna, S.; Ciofini, I.; Adamo, C. *Inorg. Chem.* **2006**, in press.
(85) Maubert, B.; McClenaghan, N. D.; Indelli, M. T.; Campagna, S. *J. Phys. Chem. A* **2003**, *107*, 447−455.
(86) Ford, W. E.; Rodgers, M. A. J *J. Phys. Chem.* **1992**, *96*, 2917−2920.
(87) Simon, J. A.; Curry, S. L.; Schmehl, R. H.; Schatz, T. R.; Piotrowiak, P.; Jin, X.; Thummel, R. P. *J. Am. Chem. Soc.* **1997**, *119*, 11012−11022.
(88) Tyson, D. T.; Castellano, F. N. *J. Phys. Chem. A* **1999**, *103*, 10955−10960.
(89) Passalacqua, R.; Loiseau, F.; Campagna, S.; Fang, Y.-Q.; Hanan, G. S. *Angew. Chem., Int. Ed.* **2003**, *42*, 1608−1611.
(90) McClenaghan, N. D.; Leydet, Y.; Maubert, B.; Indelli, M. T.; Campagna, S. *Coord. Chem. Rev.* **2005**, *249*, 1336−1350.
(91) It is known that when in multichromophoric species where luminescent metal-based MLCT triplet states are close in energy with triplet states involving organic chromophores, equilibration between the triplet states can occur.[85−90] In particular, when the rate constant of any other decay is negligible compared to the equilibration time, the lifetime of the equilibrated state is dictated by weighted linear combination of the intrinsic lifetimes of the components according to Boltzmann distribution.

lifetime would be quite longer in this case,[92] or (ii) to the lifetime of the equilibrated state.[93] We have no simple way to discriminate between the routes (i) and (ii), also considering that the LC triplet is not expected to have significant transient absorption features in comparison with the MLCT state, so the lack of changes in the transient spectrum could be misleading. It should be noted that case (i) would indicate a slow electron-transfer rate ($k_{el} \approx 6 \times 10^6$ s^{-1}) for the oxidative PET from the equilibrated state to the acceptor A subunit. However, such an electron transfer from an equilibrated state could be a complicated process, so we do not feel this is enough to rule out this decay route. In any case, as a matter of fact the primary deactivation process of the luminescent MLCT state in **4** and **5** appears to be different.

It remains to be commented the reason for the different behavior of **4** and **5** with regard to the ET/EnT quenching processes, in particular the fact that ET appears to dominate in **5** while EnT dominates in **4**, at least at an early stage. From a thermodynamic viewpoint, ET and EnT processes in **4** and **5** are in fact very similar. Also, these species virtually have the same conformation (about θ_1) on average. Basically, the dyads are only differentiated by existing *conformational locking* within **5** ensured by R^0 methyl substituents of the xylyl spacer (Charts 1 and 2), which reduce the amplitude of thermal structure fluctuations as compared to **4**. Thus, the minimized electronic coupling between the MLCT chromophore (P1/Os) and the *electron* and *energy* acceptor (A) unit is maintained *in the excited state*. Noteworthy, A is in both cases the TP^+-NO_2 moiety. The importance of electronic coupling is larger for electron exchange EnT, that is the mechanism considered to drive EnT in our systems, than for ET. Thus, it can be foreseen that EnT decay is slowed to a much larger extent than the ET process on passing from **4** to **5**. As a consequence, whereas EnT (that is, the equilibration process) is competitive in **4**, it is much less an efficient decay route in **5**. There are several examples reported in the literature in which restricted spacer conformations limit intercomponent coupling and therefore ET and/or EnT processes.[41,43,45,57,61,94,95]

Furthermore, we cannot exclude that EnT in **4** is favored by a particular planar conformation on the occasion of thermal structure fluctuations about θ_1 mean angle,[41b] while such a conformation is not possible for **5** whose intercomponent geometrical decoupling is locked.

3. Summary

We synthesized and studied a series of osmium(II)- and ruthenium(II)-based photosensitizer-electron acceptor dyads containing triarylpyridinio-functionalized (TP^+) terpyridyl ligands. Our results indicate the following:

−Planarization is apparently an efficient way of structural relaxation of MLCT states.

−A nitro substituent on the TP^+ electron acceptor subunit makes MLCT emission quenching by oxidative electron transfer to TP^+ slightly exoergonic, and indeed such a process is effective at room temperature for the *conformationally locked* compound **5**, leading to targeted CSS formation. For the *conformationally unlocked compound* **4**, fast equilibration between the MLCT and a NO_2-based LC triplets takes place (reversible EnT) and precedes ET decay with CSS formation. This finding strongly points out that excited-state relaxation and thermal structure fluctuations about *restrained* (i.e., weakly restricted) or *constrained* (i.e., strongly restricted and even locked) conformations can have pivotal roles in determining both the rate constant of the decay processes and also the dominant mechanism of the decay itself. In other words, we have evidenced here a *conformational gating of photoinduced processes*.

Beyond providing guidelines for the design of next generation of TP^+-based PMDs (toward "redox cascades"), the present work affords issues of relevance for the field of supramolecular photochemistry as aryl-substituted oligopyridine ligands are of widespread use to build complexes photosensitizers within photoactive functional arrays or supramolecular architectures.[12,96,97] Also, propensity for increasing compactness of PMDs' in view to multifunctional integration de facto correlates with the rising importance of monitoring intercomponent electronic coupling arranged by the interplay of active units with the orbitals of intervening spacer elements. Last, possible implications of conformational gating for the future regarding switching effects and sensors relying on modulation of emission lifetimes[98] must be considered.

4. Experimental Section

4.1. Syntheses, Characterization and General Experimental Details. Electronic absorption spectra were measured on a JASCO V-570 spectrophotometer. ^{1}H NMR spectra were recorded on a Bruker ARX 250 spectrometer. Elemental analyses were performed at the Institut de Chimie des Substances Naturelles, France. ESI(+) mass spectra (solvent, acetonitrile) were recorded with a LCQ-advantage (ThermoFinnigan) mass spectrometer.

4.2. Crystal Structure Determination. Suitable crystal of ligand tpy-xy-$TPH_2(NO_2)^+$ was mounted on a Bruker−Nonius KappaCCD diffractometer. Orientation matrix and lattice parameters were obtained by least-squares refinement of the reflections obtained by a θ-χ scan (Dirax/lsq method). Data were collected at 293(2) K using graphite-monochromated Mo−K_α radiation ($\lambda = 0.710\,73$ Å). A summary of the crystallographic data and structure refinement is given in Table SI-1 (Supporting Information). The indexes of data collection were $-13 \le h \le 11$, $-18 \le k \le 18$, $-17 \le l \le 20$. Of the 8997 measured independent reflections in the θ range 2.15−28.0°, 5494 have $I \ge 2\sigma(I)$. All the measured independent reflections were used in the analysis. All calculations for data reduction, structure solution, and refinement were done by standard procedures (WINGX).[99] The structure was solved by direct methods and refined with full-matrix least-squares technique on F^2 using the SHELXS-97[100] and SHELXL-97[101] programs. A careful inspection of the difference maps and subsequent refinement of the site occupation factors (sof) showed two statistical positions for the

(92) Within such an assumption, the emission lifetime of **4** would be adventitiously falling in the time scale typical for P1/Os-based luminophores when barely affected, as is the case for dyads **2** and **3**, and could be of several orders of magnitude longer in the absence of the PET process.

(93) The unquenched lifetime of the equilibrated state depends on the energy gap between the involved states and on the intrinsic lifetime of the LC (nitro-based) level at room temperature. Although we know the 77 K lifetime of the free ligands containing the nitro group (which is in the ms time scale)[84] at the moment we have no information on the room-temperature lifetime of the LC state in the complexes.

(94) Schlicke, B.; Belser, P.; De Cola, L.; Sabbioni, E.; Balzani, V. *J. Am. Chem. Soc.* **1999**, *121*, 4207−4214.
(95) Scandola, F.; Chiorboli, C.; Indelli, M. T.; Rampi, M. A. in *Electron Transfer in Chemistry*; Balzani, V., Ed.; Wiley-VCH: Weinheim, 2001; Vol. 3, p 337.
(96) (a) Hofmeier, H.; Schubert, U. S. *Chem. Soc. Rev.* **2004**, *33*, 373−399. (b) Andres, P. R.; Schubert, U. S. *Adv. Mater.* **2004**, *16*, 1043−1068.
(97) Balzani, V.; Juris, A.; Venturi, M.; Campagna, S.; Serroni, S. *Chem. Rev.* **1996**, *96*, 759−833.
(98) Higgins, B.; DeGraff, B. A.; Demas, J. N. *Inorg. Chem.* **2005**, *44*, 6662−6669.
(99) Farrugia, L. J. *WINGX, J. Appl. Crystallogr.* **1999**, *32*, 837−838.

nitrogen atom and one carbon atom of one acetonitrile molecule. The atoms of the other acetonitrile molecule were refined anisotropically with fixed occupancy factors which were established in a previous refinement with isotropic thermal factors (sof is 0.5). All hydrogen atoms were both set in calculated positions and isotropically refined. The final Fourier-difference map showed maximum and minimum height peaks of 0.627 and −0.491 e $Å^{-3}$. The final geometrical calculations and the graphical manipulations were carried out with DIAMOND[101] program.

4.3. Electrochemical and Spectroelectrochemical Measurements. The electrochemical and UV−vis. spectroelectrochemical experimental setup have been described in ref 37a. Cyclic voltammetric data were used to estimate formal potentials $E_{1/2}$ as $(E_{pa} + E_{pc})/2$ where E_{pa} and E_{pc} are the anodic and cathodic peak potentials related to the considered redox process. In some cases, $E_{1/2}$ was evaluated directly on the hydrodynamic voltammograms as being the half-wave potential value. The number n of electrons involved in the redox process was determined by (i) comparison with reference components, or (ii) with respect to the internal monoelectronic oxidation of the metal center within the examined complexes or (iii) from the value of $E_{pc}-E_{p/2}$ which is equal to $56.5/n$ mV at 25 °C for reversible redox processes (where $E_{p/2}$ is the potential value at the half peak current intensity).[102]

4.4. Photophysical Properties. For **1**−**5**, uncorrected emission spectra were obtained with a Jobin Yvon Spex Fluorolog FL 111 spectrofluorimeter ($\lambda_{exc.} = 600$ nm). For **0**, **6**, **9**, and **10**, luminescence spectra were recorded with a Spex-Jobin Yvon Fluoromax-P spectrofluorimeter equipped with a Hamamatsu R3896 photomultiplier, and were corrected for photomultiplier response using a program purchased with the fluorimeter ($\lambda_{exc.} = 450$ nm). Luminescence quantum yields for argon-degassed acetonitrile solutions of the complexes have been calculated by using the optically dilute method.[103] These quantum yields were determined relative to reference acetonitrile solutions of $[Os(bpy)_3]^{2+}$ ($\Phi_{em} = 5 \times 10^{-3}$)[104] or $[Ru(bpy)_3]^{2+}$ ($\Phi_{em} = 6.2 \times 10^{-2}$)[71] at 298 K, for Os-based and Ru-based species, respectively.

Excited-state lifetimes of **1**,[37a] **2**,[37a] **3**, and **5** were determined by laser flash spectroscopy using a nanosecond setup previously described ($\lambda_{exc.} = 308$ nm).[37a] For the luminescence lifetimes of **0**, **4**, **6**, **9**, and **10**, an Edinburgh OB 900 time-correlated single-photon-counting spectrometer was used in the ns range. As excitation sources, a Hamamatsu PLP 2 laser diode (59 ps pulse width at 408 nm) and the nitrogen discharge (pulse width, 2 ns at 337 nm) were employed.

Picosecond time-resolved experiments were performed using a previously described pump−probe setup,[105] based on the Spectra-Physics Hurricane Ti:sapphire laser source and an Ultrafast Systems Helios spectrometer. The pump pulse was generated by a frequency doubler (400 nm). The probe pulse was obtained by continuum generation on a sapphire plate (useful spectral range, 450−800 nm). The effective time resolution was ca. 300 fs, the temporal chirp over the white-light 450−750 nm range was ca. 200 fs, and the temporal window of the optical delay stage was 0−1000 ps. The decays reported in the text are best fitting values related to an analysis of the transient spectra decays performed at twenty probe wavelengths between 500 and 760 nm.

Acknowledgment. We are indebted to Dr. Carine Guyard-Duhayon, Dr. María Hernández-Molina and Lise-Marie Chamoreau for the X-ray structure determination of [tpy-xy-$TPH_2(NO_2)$](BF_4) as well as to Dr. Edmond Amouyal for the determination of emission lifetimes of **3** and **5**. The authors thank Prof. Carlo Adamo and Dr. Ilaria Ciofini for stimulating discussions. P.P.L. is grateful to the French ministry of research for financial support (ACI project no. JC4123). S.C. and C.C. also acknowledge MIUR (FIRB and PRIN projects) for funding.

Supporting Information Available: Experimental details regarding synthesis and characterization of new compounds including ^{1}H NMR spectra of **3**−**5** and **8**−**10**; a summary of the crystallographic data and structure refinement for tpy-xy-$TPH_2(NO_2)^+$ ligand (1 Table); UV−vis. spectroelectrochemical spectral changes for *xy*-$TPH_2(NO_2)^+$ upon reduction as well as for **5** and **10** upon oxidation; normalized rt and lt emission spectra of the **1**−**5** series of complexes; ultrafast differential transient absorption (TA) decays for **3**, **4** and **5**, as well as TA spectra and decays for **6**. (PDF). X-ray structural data for the tpy-xy-$TPH_2(NO_2)^+$ ligand (CIF). This material is available free of charge via the Internet at http://pubs.acs.org.

JA058357W

(100) Sheldrick, G. M. SHEL97, Programs for Crystal Structure Analysis (Release 97−2), Institüt für Anorganische Chemie der Universität, Tammanstrasse 4, D-3400 Göttingen, Germany, 1998.
(101) Brandenburg, 1999.
(102) Bard, A. J.; Faulkner, L. R. *Electrochemical Methods: Fundamentals and Applications*, Second Edition; Wiley: New York, 2001, p 213.
(103) Demas, J. N.; Crosby, G. A. *J. Phys. Chem.* **1971**, *75*, 991−1024.
(104) Kober, E. M.; Caspar, J. V.; Lumpkin, R. S.; Meyer, T. J. *J. Phys. Chem.* **1986**, *90*, 3722−3734.
(105) Chiorboli, C.; Rodgers, M. A. J.; Scandola, F. *J. Am. Chem. Soc.* **2003**, *125*, 483−491.